

Imperial College London
Department of Physics

Generalization of Floquet Theory

M.Sc. Thesis
by

Dorian Daimer

Supervisor

Dr. Florian Mintert
Imperial College London

A thesis submitted in partial fulfilment of the requirements for the
degree of Master of Physics and the Diploma of Imperial College
London.

London, 16.09.2016

Abstract

Floquet theory is and has been for many years one of the most successful approaches to the theoretical treatment of periodically driven quantum systems. In case of non-periodic driving there are however many open questions. Some generalizations of Floquet theory have been successfully applied to quasi-periodic systems and the (t, t') formalism can be used on Hamiltonians with arbitrary time-dependence but there is no rigorous mathematical framework as of yet. A generalized formula for the calculation of the time-evolution operator based on the time-independent Floquet formalism is presented and applied to three model Hamiltonians. The numerical properties of the obtained time-evolution operators are examined. Additionally the time-evolution operators are used to calculate transition probabilities, which are compared with results from numerically integrating the time-dependent Schrödinger equation.

Table of Contents

1. Introduction	1
2. State-of-the-art	3
2.1. Floquet theory	3
2.1.1. Time-evolution operator and Floquet Hamiltonian	3
2.1.2. Time-independent formalism	5
2.1.3. Generalization of Floquet formalism to arbitrary time-dependence	6
2.1.3.1. (t, t') formalism	7
2.1.3.2. Calculating the propagator within generalized Floquet theory	8
2.2. Computing the matrix exponential of a defect matrix	9
2.2.1. Interpolation of a matrix function	10
3. Application of generalized Floquet theory	13
3.1. Landau-Zehner Hamiltonian	13
3.1.1. Numerical results	15
3.2. Interaction picture Landau-Zehner Hamiltonian	18
3.2.1. Numerical results	20
3.3. Hamiltonian with Gaussian perturbation	23
3.3.1. Numerical results	24
3.4. Computational time	28
4. Conclusion and Outlook	30
A. Appendix	32
A.1. Propagator for the Landau-Zehner Hamiltonian	32
A.2. Landau-Zehner Hamiltonian in interaction picture	32

List of Figures

3.1.	Depicted is the norm of the Schrödinger equation $\ i\partial_t U(t) - H(t)U(t)\ $ for different times and different dimensions of \mathcal{K} . The system parameters were fixed as $\alpha = 1$ and $\beta = 1$. For every dimension, there is a 'breaking point' after which the norm increases exponentially. This 'breaking point' is at greater times, the greater the dimension of \mathcal{K} . . .	16
3.2.	Depicted is the dependence of the time-evolution operator on the system parameters. All calculations were done for $\dim[\mathcal{K}] = 80$. On the left α is varied and on the right it is β	17
3.3.	Comparison between transition probabilities $ \langle 1 U(t, t_0) 0\rangle ^2$ computed using the generalized Floquet formalism and conventional step-by-step integration of the time-dependent Schrödinger equation.	18
3.4.	Depicted is the norm of the Schrödinger equation $\ i\partial_t U(t) - H(t)U(t)\ $ for different times and different dimensions of \mathcal{K} . The system parameters were fixed as $\alpha = 1$ and $\beta = 1$. The norm of the Schrödinger equation immediately increases with time. There is no 'breaking point'. The greater the dimension the smaller the norm for a fixed time value however. This implies that the dimensions included in the calculations so far are too small to display the plateau seen in Fig. 3.1	20
3.5.	Depicted is the dependence of the time-evolution operator on the system parameters. All calculations were done for $\dim[\mathcal{K}] = 72$. On the left α is varied and on the right it is β	21
3.6.	Transition probabilities $ \langle 1 U(t, 0) 0\rangle ^2$ computed using the generalized Floquet formalism for the Schrödinger picture Landau-Zehner Hamiltonian and the interaction picture Landau-Zehner Hamiltonian are compared with values obtained by numerically integrating the time-dependent Schrödinger equation for the interaction picture Hamiltonian.	22
3.7.	Depicted is the norm of the Schrödinger equation $\ i\dot{U}(t) - H(t)U(t)\ $ for different times and different dimensions of \mathcal{K} . The system parameters were fixed as $\alpha = 1$ and $\omega = 5$. The norm of the Schrödinger equation immediately increases with time. There is no 'breaking point'. The greater the dimension the smaller the norm for a fixed time value however. This implies that the dimensions included in the calculations so far are again too small to display the plateau seen in Fig. 3.1. The norm never gets larger than 1, because of the Gaussian-type exponential functions. This behaviour could not be observed in Fig. 3.4, where the norm would reach values of up to 10^4	25

List of Figures

3.8.	Depicted is the dependence of the time-evolution operator on the system parameters. All calculations were done for $\dim[\mathcal{K}] = 42$. On the left α is varied and on the right it is ω	26
3.9.	Transition probabilities $ \langle 1 U(t,0) 0\rangle ^2$ computed using the generalized Floquet formalism for the Hamiltonian with a Gaussian perturbation are compared with values obtained by numerically integrating the time-dependent Schrödinger equation.	27
3.10.	Depicted is the physical time required to calculate the propagator $U(1,0)$ for the three different model Hamiltonians for various dimensions. The time increases exponentially for all three Hamiltonians. The Gaussian-Hamiltonian ('Gauss') requires the most time, while for the two Landau-Zehner Hamiltonians ('LZ' and 'LZI', for the interaction picture) the time is of the same size.	28

Acknowledgements

I am very grateful to Dr. Florian Mintert for the opportunity to work on this project as a part of his group and for all the support provided. I would also like to thank my family and friends, without whom this report could have been finished a month ago.

Declaration

With my signature, I certify that this thesis has been written by me using only the indicated resources and materials. Where i have presented data and results, the data and results are complete, genuine, and have been obtained by me unless otherwise acknowledged; where my results derive from computer programs, these computer programs have been written by me unless otherwise acknowledged. I further confirm that this thesis has not been submitted either in part or as a whole, for any other academic degree at this or another institution.

Place, Date

Signature

1. Introduction

Simulating the complete time-evolution of an arbitrary quantum system on a classical computer requires an exponential amount of computational resources [1]. This was pointed out by Feynman as early as 1984 [2]. The states of a quantum system are wave functions defined on a vectorspace, whose dimensions increase exponentially with the systems size. To bypass this problem Feynman proposed to directly simulate one quantum system using another [2]. For this to work the simulator has to obey the same dynamics/equations of motion as the system to be simulated.

Since this idea was first proposed by Feynman the experimental control and manipulation of quantum systems has progressed rapidly [3-5]. Laser induced driving allows to control chemical reactions [6] and to investigate the electronic structure of atoms [7]. Additionally suitable driving sequences grant access to otherwise unobservable phases in solid state systems [8].

Furthermore simulations with well-controlled quantum systems, such as periodically driven atomic gases, are on the rise to answer questions beyond the present analytical and computational means [9]. Hand in hand with these developments the dynamics of quantum systems under the influence of time-dependent Hamiltonians has become a point of increasing interest for various communities over the last few years.

To understand the dynamics of driven systems, solutions to the Schrödinger equation with a time-dependent Hamiltonian are required. These solutions cannot be found as straightforwardly as for the case of time-independent Hamiltonians, where the problem is only as hard as the diagonalization of the Hamiltonian in question.

For the special case of a periodically time-dependant Hamiltonian Floquet's Theorem [10] can be used to relate this problem to one with a time-independent Hamiltonian. The use of Floquet's Theorem allows to simulate time-independent systems using periodically driven systems, making them an exceptional tool for quantum simulations. This together with recent experimental advances, especially in the field of optical systems, has put driven systems on the forefront of engineered quantum mechanical systems. The Floquet approach is however almost exclusively limited to periodic driving. While some extensions to quasi-periodically driven systems, such as many-mode Floquet theory [11], have been made, the mathematical footing for these approaches is far less rigorous and many open questions remain [12].

In this thesis generalizations of the time-independent Floquet method to Hamiltonians with arbitrary time-dependence are discussed. A generalized Floquet theory is then used to calculate the propagators for three two-level model Hamiltonians from molecular physics and quantum optics.

1. Introduction

The remainder of this thesis is structured into three parts. In the first part the main theoretical aspects, Floquet theory, its generalization and an interpolation method for the calculation of the matrix exponential, needed for the understanding of the second part are introduced. The second part contains the main results of the thesis. It describes the application of the generalized Floquet formalism to the three model Hamiltonians and discusses the results of the numerical implementation. In the last part the results are summarized and an outlook is provided, pointing out further avenues of research and possibilities for optimizing the approach.

2. State-of-the-art

In this chapter the theoretical prerequisites are introduced and the state-of-the-art theory is reviewed. First the time-propagation operator and the Floquet Hamiltonian are introduced. Secondly the time-independent formalism for periodic Hamiltonians is derived using Floquet's Theorem. Afterwards an existing approach to a generalized Floquet formalism, the (t, t') formalism, for arbitrarily time-dependent Hamiltonians is reviewed. Based on these results the approach to a generalized Floquet formalism pursued in this thesis is presented. In the last section of this chapter interpolation formulas for the calculation of matrix functions of a defect matrix are derived. These formulas are the basis of the numerical implementation of the generalized Floquet formalism for the model Hamiltonians described in Chapter 3. From this point onwards all physical quantities will be given in terms of the corresponding characteristic quantities of the system, rendering them dimensionless. While we sometimes explicitly point this out it is often simply done without mentioning, especially when quantities involving \hbar are concerned.

2.1. Floquet theory

2.1.1. Time-evolution operator and Floquet Hamiltonian

The time-evolution operator $U(t, 0)$ describes the dynamics a quantum state undergoes in the time interval t . It is determined by the solution of the Schrödinger equation

$$i \frac{\partial}{\partial t} U(t, 0) = H(t) U(t, 0) \quad (2.1)$$

with the system Hamiltonian $H(t)$ and subject to the initial condition $U(0, 0) = \mathbb{1}$. The formal solution to this equation can be written as

$$\begin{aligned} U(t, 0) &= \mathcal{T}(e^{-i \int_0^t H(t') dt'}) \\ &= \mathbb{1} + \sum_{n=1}^{\infty} \frac{(-i)^n}{n!} \int_0^t dt_1 \dots dt_n \mathcal{T}(H(t_1) \dots H(t_n)) \end{aligned} \quad (2.2)$$

with the time-ordering operator

$$\mathcal{T}(A(t)B(t')) = \begin{cases} A(t)B(t') & t > t' \\ B(t')A(t) & t' > t \end{cases}$$

2. State-of-the-art

The action of \mathcal{T} in Eq. (2.2) is only given in terms of the Taylor expansion of the exponential function. This has the disadvantage, that only approximative solutions, given by the truncation of the series can be computed.

For Hamiltonians commuting with themselves at different times, $[H(t_1), H(t_2)] = 0$ for $t_1 \neq t_2$, the solution to Eq. (2.1) is of the form

$$U(t, 0) = e^{-i \int_0^t H(t') dt'}, \quad (2.3)$$

because the time-ordering operator \mathcal{T} acts trivially on the exponential.

For time-independent Hamiltonians ($H(t) = H$) Eq. (2.2) reduces to the well-known expression

$$U(t, 0) = e^{-iHt}. \quad (2.4)$$

Floquet theory [10] asserts, that Eq. (2.1) is reducible for periodic Hamiltonians $H(t+T) = H(t)$, thus treating a special case of non-commuting Hamiltonians. Reducible in this case means, that there exists a periodic unitary $U_p(t) = U_p(t+T)$ transforming the Schrödinger operator

$$K(t) = H(t) - i \frac{\partial}{\partial t} \quad (2.5)$$

to $U_p(t)K(t)U_p^\dagger = H_F - i \frac{\partial}{\partial t}$. Here $H_F = U_p(t)H(t)U_p^\dagger - iU_p(t)(\partial_t U_p^\dagger)$ describes a time-independent Hamiltonian, the so-called Floquet Hamiltonian [12].

This in turn leads to a decomposition of the time-evolution operator of the form

$$U(t, 0) = U_p^\dagger(t) e^{-iH_F t}. \quad (2.6)$$

As this decomposition is crucial for the following results, we will explain its derivation in some detail.

The discussion below closely follows the one given in [13].

Because of the periodicity of the Hamiltonian, if $U(t, 0)$ is a solution of the Schrödinger equation then so is $U(t+T, 0)$ since

$$\begin{aligned} i \frac{\partial}{\partial t} U(t+T) &= H(t+T)U(t+T) \\ &= H(t)U(t+T) \end{aligned} \quad (2.7)$$

Let us define a time-independent unitary operator $V = U^\dagger(t)U(t+T, 0)$ [13]. It is not immediately obvious that V is indeed time-independent, but it can easily be shown by computing the time derivative of V

$$\begin{aligned} i \frac{\partial}{\partial t} V &= (i \frac{\partial}{\partial t} U^\dagger(t))U(t+T) + U^\dagger(t)(i \frac{\partial}{\partial t} U(t+T)) \\ &= -U^\dagger(t)H(t)U(t+T) + U^\dagger(t)H(t)U(t+T) \\ &= 0 \end{aligned} \quad (2.8)$$

Since V is unitary, it can be written as $V = e^{-iH_F T}$, thus defining a time-independent Hamiltonian H_F [13].

2. State-of-the-art

From V we get the relation $U^\dagger(t+T) = e^{iH_F T} U^\dagger(t)$ allowing us to define a T-periodic unitary $U_p(t) = e^{-iH_F t} U^\dagger(t)$. This is the same unitary mentioned above for transforming the Schrödinger operator.

Consequently, the time-evolution operator of a periodic Hamiltonian can be written as [13]

$$U(t, 0) = U_p^\dagger(t) e^{-iH_F t}. \quad (2.9)$$

To check that $U_p(t)$ is indeed T-periodic we compute

$$\begin{aligned} U_p(t+T) &= e^{-iH_F t} e^{-iH_F T} U^\dagger(t+T) \\ &= e^{-iH_F t} V U^\dagger(t+T) \\ &= e^{-iH_F t} U^\dagger(t) U(t+T, 0) U^\dagger(t+T, 0) \\ &= (U(t) e^{iH_F t})^\dagger = U_p(t) \end{aligned} \quad (2.10)$$

as was claimed above. $U_p(t)$ has the same periodicity as the Hamiltonian and H_F is the time-independent Floquet Hamiltonian. It is easy to see that $U(0, 0) = \mathbb{1}$ is satisfied as $U_p(0) = \mathbb{1}$.

In the next subsection, the time-independent formalism for periodically driven system is derived from the above results and the use of an extended Hilbert space.

2.1.2. Time-independent formalism

It is often more convenient to work within a time independent formalism [14, 15]. To achieve this the original Hilbert space of the system \mathcal{H}_S is extended to a so-called Floquet space \mathcal{F} , where time is not treated as a parameter but as a coordinate instead [12, 15].

In this section we will describe the time-independent formalism for periodically driven systems in terms of quantum states. The eigenstates of the Floquet Hamiltonian $|\epsilon_k\rangle$ form a basis in the Hilbert space of the system [12]. Thus any initial state $|\phi(0)\rangle$ can be expressed as a linear combination of the eigenstates of the Floquet Hamiltonian. The time-dependent states $|\phi(t)\rangle = U(t, 0) |\phi(0)\rangle$ can then be written as $|\phi(t)\rangle = e^{-i\epsilon_k t} U_p^\dagger(t) |\epsilon_k\rangle$ using the decomposition of the time-evolution operator given in Eq. (2.9). Here ϵ_k denotes the eigenvalues of the Floquet Hamiltonian $H_F |\epsilon_k\rangle = \epsilon_k |\epsilon_k\rangle$ and $|u_k(t)\rangle = U_p^\dagger(t) |\epsilon_k\rangle$ are T-periodic states. Introducing these states into the Schrödinger equation results in an eigenvalue problem of the form

$$K(t) |u_k(t)\rangle = \epsilon_k |u_k(t)\rangle. \quad (2.11)$$

Because of the non-trivial action of the derivative as part of $K(t)$ the eigenvalue problem cannot be simply solved by matrix diagonalisation [13].

Treating the periodic, time-dependent functions as elements of a Hilbert space \mathcal{H}_P and expanding the original Hilbert space \mathcal{H}_S to the extended Floquet space $\mathcal{F} = \mathcal{H}_S \otimes \mathcal{H}_P$ a Fourier representation of the states in the extended Hilbert space can be adopted by associating each time-periodic vector $|u_k\rangle = \sum_n |u_k^n\rangle e^{i\omega_n t}$ with a vector [12]

$$|u_k\rangle = \sum_n |u_k^n\rangle |n\rangle. \quad (2.12)$$

2. State-of-the-art

The vectors $|n\rangle$ are orthonormal, satisfying $\langle n|m\rangle = \delta_{nm}$.

Using this Eq. (2.12) can be rewritten in terms of a time-independent eigenvalue equation

$$\mathcal{K}|u_k\rangle = \epsilon_k|u_k\rangle \quad (2.13)$$

with the infinite-dimensional operator \mathcal{K} defined on Floquet space.

Applying the same mapping, that was used for the periodic states to the Schrödinger operator one obtains [14]

$$\mathcal{K} = \sum_n H_n \otimes \mu_n + \mathbb{1} \otimes \omega \hat{n} \quad (2.14)$$

with the ladder operators $\mu_n = \sum_m |n+m\rangle\langle m|$ and the number operator $\hat{n} = \sum_n n|n\rangle\langle n|$. The time-evolution operator $U(t, 0)$ is then given by [12]

$$U(t) = \sum_n \langle n|e^{-i\mathcal{K}t}|0\rangle e^{i\omega nt}. \quad (2.15)$$

Because \mathcal{K} is infinite-dimensional exact analytical results are generally impossible to obtain. It is however possible to compute numerically exact results by truncating the extended Hilbert space.

2.1.3. Generalization of Floquet formalism to arbitrary time-dependence

In this section the time-independent approach from Section 2.1.2 is generalized to Hamiltonians with arbitrary time-dependence. In the first part the so-called (t, t') formalism developed by Howland [16] is presented. Within the (t, t') formalism the time-dependent Schrödinger equation is solved as a time-independent problem in a generalized Hilbert space similar to the procedure in Section 2.1.2. In the generalized Hilbert space time is treated as an additional coordinate, instead of a variable. This allows determining the propagator $U(t, 0)$ without the need to perform a step-by-step integration as would be required by the time-ordering operator. For periodic Hamiltonians this approach was first developed by Sambe [15] and is discussed in the previous section. In the second part the ideas incorporated in the (t, t') formalism are used to derive an expression for the propagator of a time-dependent Hamiltonian, similar to Eq. (2.15). The ideas from this section were the starting point for this project and in the second part of this thesis the formalism from this section will be applied to several time-dependent Hamiltonians to investigate the numerical properties and the practical usefulness.

2. State-of-the-art

2.1.3.1. (t,t') formalism

Throughout this section we use the convention

$$|\Psi(t)\rangle = \Psi(x, t) \quad (2.16)$$

where x characterizes the spatial dependence of the wave function as well as any possible spin degrees of freedom. Let us consider the general time-dependent Schrödinger equation

$$i \frac{\partial}{\partial t} |\Psi(t)\rangle = H(t) |\Psi(t)\rangle \quad (2.17)$$

with the given initial state

$$|\Psi(t = t_0)\rangle = |\Psi(t_0)\rangle. \quad (2.18)$$

The time-dependent solution of Eq. (2.17) is formally given by

$$|\Psi(t)\rangle = U(t, t_0) |\Psi(t_0)\rangle. \quad (2.19)$$

The solution of the explicitly time-dependent Schrödinger equation can also be obtained as [17,18]

$$|\Psi(t)\rangle = |\Psi(t, t')\rangle|_{t'=t} \quad (2.20)$$

where

$$|\Psi(t, t')\rangle = \exp\left(-i(H(t') - i \frac{\partial}{\partial t'})(t - t_0)\right) |\Psi(t_0, t')\rangle. \quad (2.21)$$

Here the time t' acts as an auxillary coordinate in a generalized Hilbert space first introduced by Sambe [15] and Howland [16]. The generalized Hilbert space contains all possible square integrable functions of coordinates x and t' [17]. Box normalisation of length T is used for t' ($0 < t' < T$). This allows to define an inner product on the composite Hilbert space \mathcal{F} . For two functions $|\phi_i\rangle$ and $|\phi_j\rangle$ from \mathcal{F} the inner product is [18]

$$\langle \phi_i | \phi_j \rangle = \frac{1}{T} \int_0^T dt' \int_{-\infty}^{\infty} dx \phi_i^*(x, t') \phi_j(x, t'). \quad (2.22)$$

It remains to be shown, that Eq. (2.20) with $|\Psi(t, t')\rangle$ given by Eq. (2.21) truly solves the time-dependent Schrödinger equation. To see this we consider the time derivative of Eq. (2.21) [18]

$$\begin{aligned} i \frac{\partial}{\partial t} |\Psi(t, t')\rangle &= (H(t') - i \frac{\partial}{\partial t'}) e^{(-i(H(t') - i \frac{\partial}{\partial t'})(t - t_0))} |\Psi(t_0, t')\rangle \\ &= H(t') |\Psi(t, t')\rangle - i \frac{\partial}{\partial t'} |\Psi(t, t')\rangle. \end{aligned} \quad (2.23)$$

Reordering then gives

$$i \left(\frac{\partial}{\partial t} + \frac{\partial}{\partial t'} \right) |\Psi(t, t')\rangle = H(t') |\Psi(t, t')\rangle. \quad (2.24)$$

Now since there is only one physical time and t' was introduced as an auxillary coordinate of the generalized Hilbert space for the final, physical result we are interested

2. State-of-the-art

only in the contour on which $t'=t$ and thus the distinction between the two different time variables vanishes. On the contour in question we have $\partial t'/\partial t = 1$ and thus [17,18]

$$\frac{\partial |\Psi(t, t')\rangle}{\partial t'} \Big|_{t'=t} + \frac{\partial |\Psi(t, t')\rangle}{\partial t} \Big|_{t'=t} = \frac{\partial |\Psi(t)\rangle}{\partial t}. \quad (2.25)$$

This result when combined with Eq. (2.24) for $t'=t$ proves the above claim and shows that Eq. (2.20) indeed solves the time-dependent Schrödinger equation (Eq. (2.17)).

2.1.3.2. Calculating the propagator within generalized Floquet theory

The goal of this section is to derive a generalization of Eq. (2.15) for Hamiltonians $H(t)$ with arbitrary time-dependence¹. While in the previous section we found a solution of the time-dependent Schrödinger equation in terms of state vectors, we will now do the same in terms of the propagator. The approach introduced here is very similar to the one from the previous section. Therefore some of the results we derive in this section were already implicitly included in Sec. 2.1.3.1. Nonetheless, it is instructive to see the problem tackled from a slightly different angle. Furthermore the results from this section form the theoretical basis for the results presented in the following parts of this thesis.

Let us denote the time-dependent functions contained in $H(t)$ by $f_i(t)$. Further we denote the space containing the $f_i(t)$, products of these functions and their derivatives as well as the constant function 1 by \mathcal{T} . We can consider the operator

$$\mathcal{V} = \exp \left(-i \left(H(t') - i \frac{\partial}{\partial t'} \right) t \right) \quad (2.26)$$

as an operator acting on the composite Hilbert space $\mathcal{H}_S \otimes \mathcal{T} \otimes \mathcal{T}'$, here \mathcal{T} and \mathcal{T}' denote the space of functions of variables t and t' respectively and \mathcal{H}_S is the system Hilbert space. In the previous section this operator was already implicitly introduced in Eq. (2.21).

Let us define the linear map

$$\Gamma : (\mathcal{B}(\mathcal{T}') \otimes \mathcal{B}(\mathcal{T})) \rightarrow \mathcal{T} \quad (2.27)$$

with

$$\Gamma(A(t') \otimes B(t)) = A(t)B(t)1, \quad (2.28)$$

here $\mathcal{B}(t)$ denotes the set of (bound) operators acting on \mathcal{T} and $A(t') \in \mathcal{B}(\mathcal{T}')$.

The map satisfies

$$\frac{\partial}{\partial t} \Gamma(X) = \Gamma \left(\left(\frac{\partial}{\partial t'} + \frac{\partial}{\partial t} \right) X \right) \quad (2.29)$$

¹This description was first devised by Florian Mintert and was graciously made available for this project.

2. State-of-the-art

since

$$\begin{aligned}\frac{\partial}{\partial t}\Gamma(A(t') \otimes B(t)) &= \frac{\partial}{\partial t}(A(t)B(t)1) = (\dot{A}B + A\dot{B})1 \\ &= \Gamma\left(\frac{\partial A(t')}{\partial t'} \otimes B(t) + A(t') \otimes \frac{\partial B(t)}{\partial t}\right).\end{aligned}\quad (2.30)$$

The map Γ is a generalization of the map $\sum_n \langle n | \cdot | 0 \rangle e^{i\omega n t}$ used for periodic Hamiltonians in Sec. 2.1.2.

Now it remains to be shown that

$$U(t, 0) = \Gamma(\mathcal{V}) \quad (2.31)$$

satisfies the Schrödinger equation

$$\begin{aligned}i\frac{\partial}{\partial t}\Gamma(\mathcal{V}) &= i\Gamma\left(\left(\frac{\partial}{\partial t'} - i\left(H(t') - i\frac{\partial}{\partial t'}\right)\right)\mathcal{V}\right) \\ &= \Gamma(H(t')\mathcal{V}) \\ &= \Gamma(H(t')(\sum_j A_j(t') \otimes B_j(t))) \\ &= \sum_j \Gamma(H(t')A_j(t') \otimes B_j(t)) \\ &= \sum_j (H(t)A_j(t)B_j(t))1 \\ &= H(t)\sum_j (A_j(t)B_j(t)) \\ &= H(t)\Gamma(\mathcal{V}).\end{aligned}\quad (2.32)$$

To derive the final result we made use of the decomposition of $\mathcal{V}(t, t') = \sum_j A_j(t') \otimes B_j(t)$. Also, $\Gamma(\mathcal{V})|_{t=0} = \mathbb{1}$ is satisfied.

2.2. Computing the matrix exponential of a defect matrix

To compute the time-evolution operator it is necessary to compute the matrix exponential of the transformed, time-independent Schrödinger operator \mathcal{K} . The transformed Schrödinger operator is in principle infinite dimensional but in order to compute numerical results the Hilbert space is truncated, leading to a finite dimensional operator. Due to the time-dependence of the Hamiltonian and the action of the derivative, \mathcal{K} is in general not diagonalizable, meaning that the matrix exponential cannot simply be computed by exponentiating the eigenvalues of \mathcal{K} . Instead we make use of interpolation [19,20].

2. State-of-the-art

2.2.1. Interpolation of a matrix function

We will first treat the case of distinct eigenvalues and later generalize this to non-distinct eigenvalues.

Let \mathcal{A} be a $n \times n$ -dimensional matrix with n distinct eigenvalues λ_i , $i = 1, \dots, n$ and let $f(\cdot)$ be the function of interest. If the eigenvalues are all lying within the circle of convergence of $f(z)$ ($z \in \mathbb{C}$), then the matrix function $f(\mathcal{A})$ is given by [21]

$$f(\mathcal{A}) = \sum_{i=1}^n f(\lambda_i) \prod_{j=1, j \neq i}^n \frac{\mathcal{A} - \lambda_j \mathbb{I}}{\lambda_i - \lambda_j}. \quad (2.33)$$

While the above formula works for general $f(\cdot)$, we are only interested in the matrix exponential for the purposes of this thesis. All the results from this section will however be derived for general functions for the sake of mathematical completeness. It should be pointed out, that the circle of convergence for the exponential function encompasses the complete complex plane and will thus always include all eigenvalues of the matrix in question. To prove Eq. (2.33) a modification of the Theorem of Friedman is used [22].

Theorem 2.2.1 *Let $p(z)$ be a polynomial with distinct roots and $f(z)$ a function analytic in a domain \mathcal{D} , containing the roots of $p(z)$. Then there exists a unique polynomial $r(z)$ ($\deg(r) = \deg(p) - 1$) and a function $h(z)$ analytic in \mathcal{D} such that*

$$f(z) = p(z)h(z) + r(z) \quad (2.34)$$

To prove the above theorem let us denote the roots of $p(z)$ with λ_i , $i = 1, \dots, n$ with $\lambda_i = \lambda_j \Leftrightarrow i = j$. For $r(z)$ take the Lagrange interpolating polynomial [23]

$$r(z) = \sum_{i=1}^n f(\lambda_i) \prod_{j=1, j \neq i}^n \frac{z - \lambda_j}{\lambda_i - \lambda_j}. \quad (2.35)$$

The Lagrange interpolating polynomial has the special property, that it agrees with $f(z)$ at each λ_i [23]. Reordering Eq. (2.34) gives

$$h(z) = \frac{f(z) - r(z)}{p(z)}. \quad (2.36)$$

The polynomial $p(z)$ is zero only for $z = \lambda_i$, but in this case the numerator in Eq. (2.36) is also zero. This means that $h(z)$ has only removable singularities

$$\lim_{z \rightarrow \lambda_i} (z - \lambda_i)h(z) = 0. \quad (2.37)$$

Thus $h(z)$ is analytic in the domain \mathcal{D} and the above theorem holds.

To get the matrix function $f(\mathcal{A})$ let $p(\cdot)$ be the characteristic polynomial of \mathcal{A} .

2. State-of-the-art

The Cayley-Hamilton theorem [24] states that \mathcal{A} solves its own characteristic polynomial thus we have $p(\mathcal{A}) = 0$ and Eq. (2.34) reduces to $f(\mathcal{A}) = r(\mathcal{A})$ with $f(\lambda_i) = r(\lambda_i), i = 1, \dots, n$. This is a linear system, giving the coefficients of $r(z)$. The Lagrange interpolating polynomial satisfies all the conditions $f(\lambda_i) = r(\lambda_i), i = 1, \dots, n$. So

$$f(\mathcal{A}) = r(\mathcal{A}) = \sum_{i=1}^n f(\lambda_i) \prod_{j=1, j \neq i}^n \frac{\mathcal{A} - \lambda_j \mathbb{1}}{\lambda_i - \lambda_j} \quad (2.38)$$

as claimed in the beginning. This formula is often referred to as Sylvester interpolation formula.

While the above discussion relied on \mathcal{A} having n distinct eigenvalues it is straightforward to generalize the results to non-distinct eigenvalues [25,26].

Theorem 2.2.2 *Let $p(z)$ be a polynomial of degree n with k distinct roots ($k < n$) and let $f(z)$ be a function analytic in a domain \mathcal{D} containing the roots of $p(z)$. Then there exists a unique polynomial $q(z)$ with $\deg q = \deg p - 1$ and a function $h(z)$ analytic in \mathcal{D} so that*

$$f(z) = p(z)h(z) + q(z) \quad (2.39)$$

holds as in theorem 2.2.1.

It should be pointed out here that the analyticity of $f(z)$ is not strictly necessary for the proof but we require it to make the switch between complex arguments and matrix arguments mathematically unproblematic [27].

Let us prove theorem 2.2.2.

Again we denote the distinct roots of $p(z)$ with $\lambda_i, i = 1, \dots, k$. The multiplicity of each root being m_i , we have $\sum_{i=1}^k m_i = n$. We require $r(z)$ to be the polynomial of degree $n - 1$ that agrees with $f(z)$ at each λ_i and whose derivatives of all orders up to $m_i - 1$ agree with those of $f(z)$ at each λ_i

$$f^{(j)}(\lambda_i) = q^{(j)}(\lambda_i), \quad j = 0, 1, \dots, m_i - 1, i = 1, \dots, k. \quad (2.40)$$

Then $q(z)$ exists and is unique, it is in fact a form of the general Hermite oscillating polynomial [27]. Reordering Eq. (2.39) gives

$$h(z) = \frac{f(z) - q(z)}{p(z)}. \quad (2.41)$$

Each root λ_i of $p(z)$ is a zero of order m_i of the denominator of $h(z)$. Applying L'Hospital's rule m_i -times to $h(z)$ for each λ_i gives

$$\lim_{z \rightarrow \lambda_i} h(z) = \lim_{z \rightarrow \lambda_i} \frac{f^{(m_i)}(z) - q^{(m_i)}(z)}{p^{(m_i)}(z)} < \infty \quad \forall i. \quad (2.42)$$

Thus $h(z)$ is analytic within the domain \mathcal{D} and Eq. (2.39) holds. We ensured that we could make use of L'Hospital's rule by requiring $r(z)$ to fulfil Eq. (2.40).

2. State-of-the-art

The matrix exponential is again computed by using the characteristic polynomial of \mathcal{A} for $p(z)$ giving again

$$f(\mathcal{A}) = q(\mathcal{A}), \quad (2.43)$$

or if $q(\mathcal{A})$ is written out explicitly [20]

$$f(\mathcal{A}) = \sum_{i=1}^k \left[\sum_{j=0}^{m_i-1} \left(\frac{1}{j!} \frac{\partial^j}{\partial \lambda_i^j} \left(\frac{f(\lambda_i)}{\prod_{p \neq i} (\lambda_i - \lambda_p)} \right) (\mathcal{A} - \lambda_i \mathbb{I})^j \right) \prod_{q \neq i} (\mathcal{A} - \lambda_q \mathbb{I})^{m_q} \right]. \quad (2.44)$$

This formula is often called the Hermite interpolating formula.

3. Application of generalized Floquet theory

In this chapter we will apply the time-independent formalism developed in Sec. 2.1.3.1 and Sec. 2.1.3.2 to three model Hamiltonians from molecular and atomic physics and use this to compute the time-evolution operator $U(t, t_0)$. The numerical behaviour of the time-evolution operator is analysed and the dynamical behaviour of the systems is studied.

The general procedure is the same for all three model Hamiltonians. First the Schrödinger operator $K(t) = H(t) - i\frac{\partial}{\partial t}$ is transformed into a time-independent operator \mathcal{K} on the extended Hilbert space, consisting of the system Hilbert \mathcal{H}_S and the space of time-dependent functions, $f_i(t)$, \mathcal{T} . Then the time-propagation operator is calculated using a generalization of Eq. (2.15). Once the time-evolution operator is obtained the dynamics of the system can be calculated and compared with the results of a step-by-step integration of the time-dependent Schrödinger equation. Additionally the numerical behaviour and stability as well as the dependence of the time-evolution operator on the system (control) parameters is studied. All systems considered are two-level systems.

3.1. Landau-Zehner Hamiltonian

The first Hamiltonian under consideration is a so-called Landau-Zehner Hamiltonian [28,29]

$$H(t) = \beta\sigma_x + \alpha t\sigma_z, \quad (3.1)$$

consisting of a time-independent part and a time-dependent energy separation.

Here $\sigma_{x,y,z}$ denote the three Pauli matrices and α and β are parameters of the system. Landau-Zehner Hamiltonians commonly occur in molecular physics, when one considers transitions between two energy bands [29]. Adiabatically the transition probability is zero, but non-adiabatic transitions between the two bands are possible [29]. The time-dependent part of the Landau-Zehner Hamiltonian is linearly time-dependent, therefore it serves as a good starting point to test the time-independent formalism.

Let us introduce the Floquet space $\mathcal{F} = \mathcal{H}_S \otimes \mathcal{T}$, arising from the extension of the Hilbert space of the system \mathcal{H}_S to the space of time-dependent polynomials \mathcal{T} . The functions $f_n(t) = t^n$ can be associated with vectors $|f_n\rangle$ ($|f_n\rangle \in \mathcal{T}$) to form a

3. Application of generalized Floquet theory

basis of \mathcal{T} . These functions are also sufficient to describe the time-dependence of the Hamiltonian, which can be written as

$$H(t) = \sum_m f_m(t) \mathcal{H}_m. \quad (3.2)$$

Here \mathcal{H}_m denote the time-independent operators and $f_m(t)$ denote the time-dependent functions. For the Landau-Zehner Hamiltonian introduced above the time-dependent functions are polynomials in t . In Floquet space time is treated as a coordinate rather than a parameter and it can thus be eliminated from the problem, rendering it effectively time-independent. The Schrödinger operator is given by $K(t) = H(t) - i \frac{\partial}{\partial t}$. For the time-independent approach it is essential to transform this operator to a time-independent operator on Floquet space \mathcal{F} . Let the transformed Schrödinger operator be called \mathcal{K} . By considering the action of the time-dependent term of $H(t)$ and the derivative operator on the basis states of \mathcal{T} ,

$$t f_n(t) = f_{n+1}(t) \quad \text{and} \quad \frac{\partial}{\partial t} f_n(t) = n f_{n-1}(t), \quad (3.3)$$

the time-independent Schrödinger operator can be computed as

$$\mathcal{K} = \beta \sigma_x \otimes \mathbb{1} + \alpha \sigma_z \otimes b^\dagger - i \mathbb{1} \otimes a. \quad (3.4)$$

This is a time-independent operator acting on Floquet space. b^\dagger and a denote a type of raising and lowering operators respectively, acting on \mathcal{T} and satisfying $b^\dagger |f_n\rangle = |f_{n+1}\rangle$ as well as $a |f_n\rangle = n |f_{n-1}\rangle$ as required by Eq. (3.2). This definition also allows for a definition of the number operator $\hat{n} = b^\dagger a$ with $\hat{n} |f_n\rangle = n |f_n\rangle$. Let us denote the matrix exponential of \mathcal{K} with \mathcal{V} , following the notation introduced in Sec. 2.1.3.2

$$\mathcal{V} = e^{-i\mathcal{K}t}. \quad (3.5)$$

Once this is done, the time-evolution operator $U(t)$ can be computed as

$$U(t, 0) = \sum_n f_n(t) \langle f_n | \mathcal{V} | f_0 \rangle. \quad (3.6)$$

This is an operator acting on the Hilbert space of the system only. In the appendix (Sec. (A.1)), we show, that $U(t)$ defined in this way satisfies the time-dependent Schrödinger equation for the Landau-Zehner Hamiltonian introduced in Eq. (3.1). The initial condition $U(0) = \mathbb{1}$ results directly from $\sum_n f_n(t) \langle f_n | e^{-i\mathcal{K}0} | f_0 \rangle = f_0 \mathbb{1} = \mathbb{1}$. Eq. (3.6) closely resembles Eq. (2.15) where the complex exponential functions have been exchanged for the time-dependent functions $f_n(t)$ introduced in Eq. (3.2). The time derivative of the propagator is given by

$$\frac{\partial}{\partial t} U(t, 0) = \sum_n \left(\frac{\partial f_n(t)}{\partial t} \langle f_n | \mathcal{V} | f_0 \rangle + f_n(t) \langle f_n | -i\mathcal{K} \mathcal{V} | f_0 \rangle \right). \quad (3.7)$$

To test the above formalism Eq. (3.6) and Eq. (3.7) have been implemented in Mathematica (Version 11). While \mathcal{K} is an infinitely dimensional operator acting on \mathcal{F} it is

3. Application of generalized Floquet theory

necessary to work with a truncated Hilbert space to get numerical results. Also \mathcal{K} is a non-hermitian operator, meaning, that it is not possible to simply diagonalize it to compute the matrix exponential. Instead, the interpolating formulas introduced in Sec. 2.2 are used to calculate the matrix exponential. To test that the implemented operators were correct, we first used a Taylor expansion for Eq. (3.5) and checked whether Eq. (3.6) satisfied the time-dependent Schrödinger equation for small times and up to the order of the Taylor expansion. This was done for all three model Hamiltonians and only after the results were satisfactory did we implement the interpolation formulas.

As a measure of quality we used the norm of the Schrödinger equation $\|i\dot{U}(t) - H(t)U(t)\|$. If the norm is much smaller than 1 even for large times it is a good indication, that the generalized Floquet formalism can be used to treat systems with arbitrary time-dependence. However this method is not foolproof, as we will see in Sec. 3.3.1. Additional quality checks should be included.

In the next section we will examine the numerical dependence of the propagator on the truncation of the Hilbert space and the systems parameters. Additionally we will present transition rates computed with the above formalism and compare them with transition rates computed with the conventional step-by-step integration of the time-dependent Schrödinger equation.

3.1.1. Numerical results

In this section the results of the implementation of the generalized Floquet formalism for the Landau-Zehner Hamiltonian are discussed. For the Schrödinger operator introduced in Eq. (3.4), Sylvester interpolation (Eq. (2.33)) is sufficient as the multiplicity of every eigenvalue is equal to one. For the other two model Hamiltonians Hermite interpolation (Eq. (2.44)) has to be used. Let us first focus on the influence of the necessary truncation of the Hilbert space. For this the system parameters α and β are left constant and the propagator as well as its derivative are calculated for times from $t = -2$ to $t = 2$. The initial time is always taken to be $t_0 = 0$. At this point it should be mentioned, that all times are given in terms of the characteristic time τ of the system and are thus dimensionless. The characteristic time of the two-level system is determined by the inverse frequency of the system, which in turn is determined by the energy separation between the levels, $\tau = \frac{2\pi}{\omega}$, with energy separation $\delta E = \omega$. The same is done for the system parameters, which are given in terms of the fundamental energy scale of the system.

3. Application of generalized Floquet theory

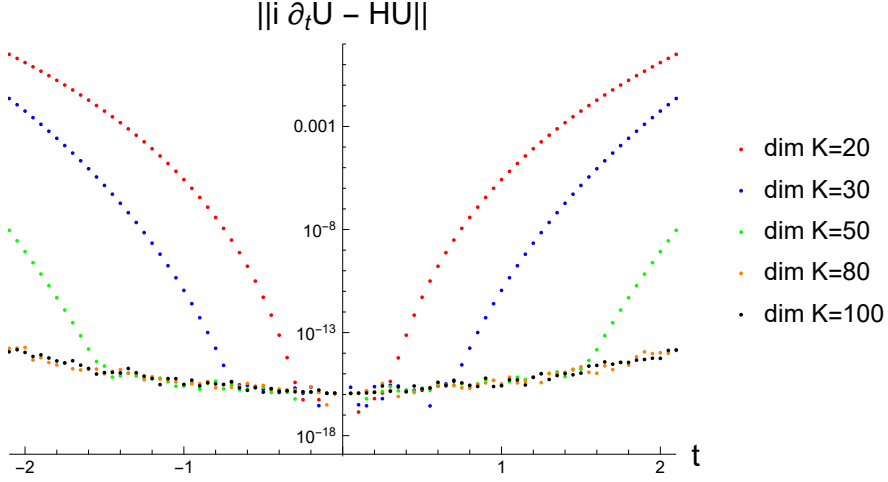


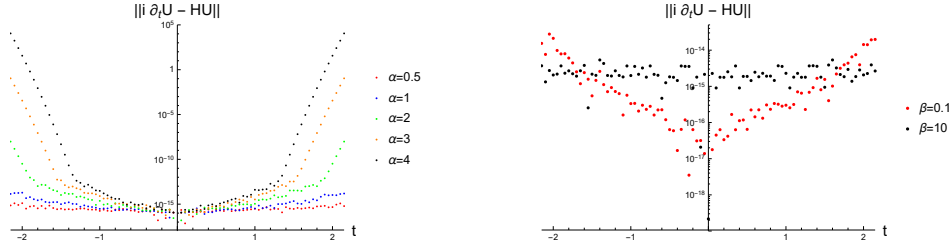
Figure 3.1.: Depicted is the norm of the Schrödinger equation $\|i\partial_t U(t) - H(t)U(t)\|$ for different times and different dimensions of \mathcal{K} . The system parameters were fixed as $\alpha = 1$ and $\beta = 1$. For every dimension, there is a 'breaking point' after which the norm increases exponentially. This 'breaking point' is at greater times, the greater the dimension of \mathcal{K} .

In the above figure the norm $\|i\dot{U}(t) - H(t)U(t)\|$ is shown for various dimensions of the operator \mathcal{K} . For this analysis the system parameter were not varied but fixed as $\alpha = 1$ and $\beta = 1$ in order to examine only the influence of the truncation. As expected the error is negligible for small times. For every dimension there seems to be a 'breaking point' in time after which the error exponentially increases and the propagator satisfies the Schrödinger equation less and less well. This 'breaking point' is higher the greater the dimension of \mathcal{K} . This behaviour is reasonable as the truncation inevitably introduces an error and this error is smaller the bigger the part of the Hilbert space included in the calculations. However there is always a trade-off between precision and computational resources. The more dimensions are included the longer it takes to find all the eigenvalues of \mathcal{K} needed for the interpolation of the matrix exponential. A detailed discussion of the computational time is given in Sec. 3.4 after all the model Hamiltonians have been introduced and discussed. We want to mention at this point already that the computational time needed increases exponentially with the dimension, which is a big drawback.

Another important factor is the influence of the system parameters on the calculations. While β can be varied without significantly affecting the numerical accuracy, α has a large influence on the results.

To test the dependence of the propagator on α we used a dimension of 80 for \mathcal{K} and fixed $\beta = 1$. As one can see in Fig. 3.2(a) the error increases dramatically with α . This is problematic as the interesting regime is given by $|\alpha t| \gg \beta$, meaning that the time-dependent term dominates the Hamiltonian. In this regime one expects the transition probability $|\langle 1|U(t)|0\rangle|^2$ to become constant as the σ_z term dominates,

3. Application of generalized Floquet theory



(a) The dependence of the propagator $U(t)$ on different values of α is examined. The second parameter is fixed ($\beta = 1$). The smaller the value of α , the later does the 'breaking point' occur. This implies that the generalized Floquet formalism is best suited for the treatment of a small time-dependent term. The interesting time-regime however is given by $|\alpha t| \gg \beta$.

(b) The dependence of the propagator $U(t)$ on different values of β is examined. The second parameter is fixed ($\alpha = 1$). While α has a strong influence on the quality of the propagator, β has no noticeable influence on the norm of the Schrödinger equation, which is basically the same for the whole range of $\beta \in [0.1, 15]$.

Figure 3.2.: Depicted is the dependence of the time-evolution operator on the system parameters. All calculations were done for $\dim[\mathcal{K}] = 80$. On the left α is varied and on the right it is β .

making transitions impossible. While this behaviour can be divined from the plots of the transition rate, a constant transition rate is never actually reached for the parameter regimes accessible so far. The formalism works best as long as $\beta\sigma_x$ is the dominating term. In this case however both Taylor expansion as well as perturbation theory can be used to treat the time-dependent term and are computationally far less costly than the interpolation method. These approximations break down even faster than the time-independent formalism once $|\alpha t| \approx \beta$. β determines the absolute size of the transition probability and the frequency of oscillation between ground and excited state. The larger β , the faster the oscillation between the two states. This behaviour is reasonable as $\beta\sigma_x$ is the term enabling the transition between the states. It should also be mentioned, that increasing β allows to use larger values for α , leading to the assumption that the error is dependent not on the parameters them self but on their ratio $\frac{\alpha}{\beta}$. The first tests of this assumption were negative however as $\frac{\alpha}{\beta} = \frac{1}{1/10}$ works very well whereas $\frac{\alpha}{\beta} = \frac{10}{1}$ gives completely unphysical results.

In the last part we calculated the transition probabilities for different values of α and β and compared them with the results of the numerical integration of the time-dependent Schrödinger equation. The results are depicted in Fig.3.3. We used a dimension of 80 for \mathcal{K} in these calculations.

3. Application of generalized Floquet theory

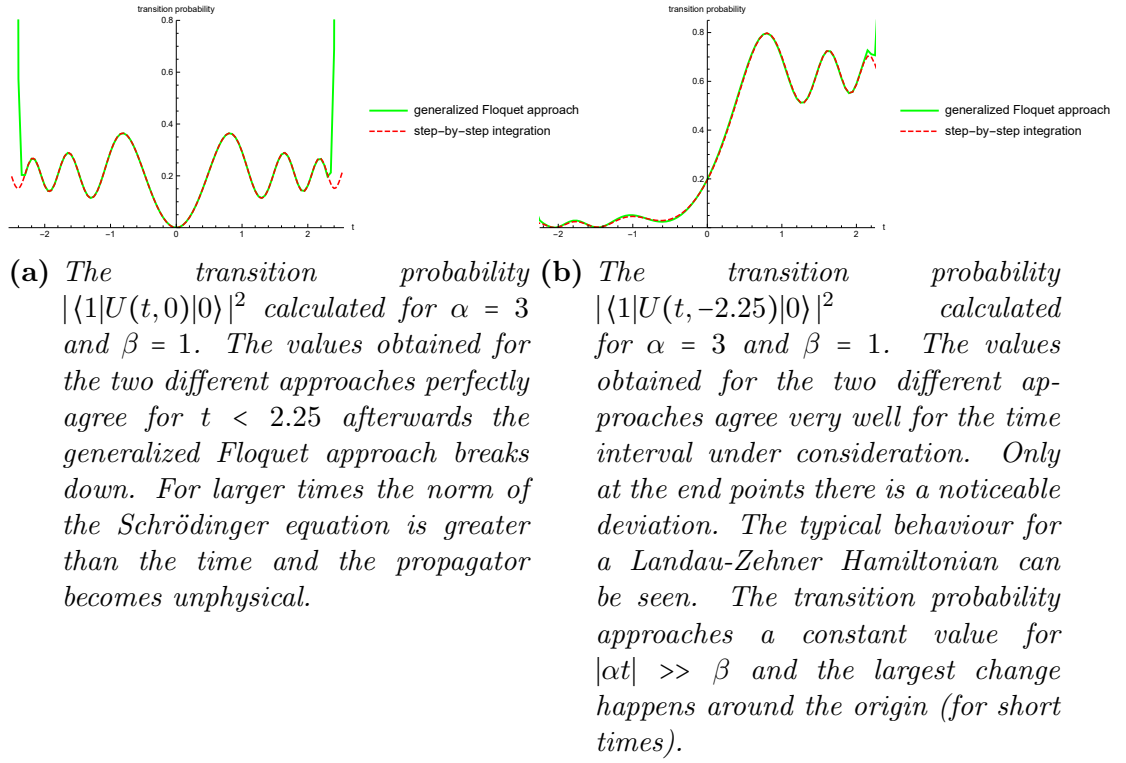


Figure 3.3.: Comparison between transition probabilities $|\langle 1|U(t,t_0)|0\rangle|^2$ computed using the generalized Floquet formalism and conventional step-by-step integration of the time-dependent Schrödinger equation.

The numerical integration agrees very well with the results from the time-independent formalism. For the time interval $t \in [-2.25, 2.25]$ the difference between the two different approaches is never greater than 10^{-6} . If one however considers a larger time interval ($t \in [-2.5, 2.5]$) the transition probabilities start to deviate as the 'breaking point' for the chosen parameter values is reached and the norm of the Schrödinger equation becomes greater than the time value.

The propagator used for the calculation of the transition rates depicted in Fig. 3.3(b) is calculated using

$$U(t_1, t_0) = U(t_1, 0)U^\dagger(t_0, 0). \quad (3.8)$$

3.2. Interaction picture Landau-Zehner Hamiltonian

The second model Hamiltonian we consider is again the Landau-Zehner Hamiltonian, but this time in its interaction picture representation

$$H_I(t) = \frac{\beta}{2}(\sigma_+ e^{2i\alpha t^2} + \sigma_- e^{-2i\alpha t^2}), \quad (3.9)$$

with $\sigma_\pm = \sigma_x \pm i\sigma_y$. The derivation of the interaction picture Hamiltonian can be found in the appendix (Sec. A.2). To treat this Hamiltonian within the time-independent

3. Application of generalized Floquet theory

formalism let us again introduce the extended Hilbert space $\mathcal{F} = \mathcal{H}_S \otimes \mathcal{T}'$. This time however the time-dependent functions associated with the Hamiltonian are not polynomials in t but instead of the form $f_{pq}(t) = t^p e^{iq\alpha t^2}$, $p \in \mathbb{N}$ and $q \in \mathbb{Z}$. The Hamiltonian can be decomposed as $H_I(t) = \sum_{p=0}^{\infty} \sum_{q=-\infty}^{\infty} f_{pq}(t) \mathcal{H}$, with the time-dependent functions $f_{pq}(t)$ introduced above and the time-independent operators H_{pq} .

We define our space of time-dependent functions \mathcal{T}' accordingly. The time-dependent functions $f_{pq}(t)$ are associated with vectors $|f_{pq}\rangle$ of \mathcal{T}' such that the vectors again form a basis in \mathcal{T}' .

Once this is done, the rest of the procedure is similar to the treatment of the Schrödinger picture Hamiltonian. The difference between the two Hamiltonians being the different time-dependent functions. The system dynamics for both Hamiltonians disregarding numerical errors should be identical as they describe the same physical process.

Let us again introduce the Schrödinger operator $K(t) = \frac{\beta}{2}(\sigma_+ e^{2i\alpha t^2} + \sigma_- e^{-2i\alpha t^2}) - i \frac{\partial}{\partial t}$ and its transformed version \mathcal{K} ,

$$\mathcal{K} = \frac{\beta}{2}(\sigma_+ \otimes a_q^\dagger + \sigma_- \otimes a_q) - i \mathbb{1} \otimes (a_p + 4 i \alpha b_p^\dagger). \quad (3.10)$$

Let us clarify the notation used for the raising and lowering operators acting on the elements of \mathcal{T}'

$$\begin{aligned} a_q |f_{pq}\rangle &= |f_{p(q-1)}\rangle \\ a_q^\dagger |f_{pq}\rangle &= |f_{p(q+1)}\rangle \\ a_p |f_{pq}\rangle &= p |f_{(p-1)q}\rangle \\ b_p^\dagger |f_{pq}\rangle &= q |f_{(p+1)q}\rangle. \end{aligned} \quad (3.11)$$

The above operators are again defined in accordance with the action of the time-dependent parts of the Hamiltonian and the time-derivative operator on the time-dependent functions $f_{pq}(t)$:

$$\begin{aligned} e^{-2i\alpha t^2} f_{pq}(t) &= f_{p(q-1)}(t) \\ e^{2i\alpha t^2} f_{pq}(t) &= f_{p(q+1)}(t) \\ \frac{\partial}{\partial t} f_{pq}(t) &= p f_{(p-1)q}(t) + 4 i \alpha q f_{(p+1)q}(t). \end{aligned} \quad (3.12)$$

Once the time-independent Schrödinger operator has been determined, we use it to compute the matrix exponential $\mathcal{V} = e^{-i\mathcal{K}t}$ and use this to calculate the time-evolution operator

$$U(t) = \sum_{pq} f_{pq}(t) \langle f_{pq} | \mathcal{V} | f_{00} \rangle. \quad (3.13)$$

In the following section we examine the behaviour of the time-evolution operator calculated using Eq. (3.13) and compare the results to the ones obtained for the Schrödinger picture Landau-Zehner Hamiltonian.

3. Application of generalized Floquet theory

3.2.1. Numerical results

As before we first discuss the influence of the truncation of the Hilbert space and afterwards the influence of the system parameters. In the end we compare the transition rates to transition rates computed for the Schrödinger picture Hamiltonian. In theory the two transition rates should agree but we will see, that numerically this is only true for small times (depending on α).

To be able to compare the results with the results obtained in Sec. 3.1.2 we again fix the system parameters as $\alpha = 1$ and $\beta = 1$ and vary the dimension of \mathcal{K} . The parameters are given in terms of characteristic system quantities, same as for the Schrödinger picture Hamiltonian (see Sec. 3.1.2). Whereas the time-dependent functions for the Schrödinger picture Hamiltonian depend on one index only, two indices are required in this case, meaning that the truncation has to be done for both. We did this by defining a parameter y and including all indices p and q , satisfying $p + |q| \leq y$ in the calculations. For every value of y we therefore include y^2 different elements of \mathcal{T}' and the same number of time-dependent functions in our calculations. The dimension of \mathcal{K} is then given by $\dim[\mathcal{K}] = 2 \cdot y^2$ as the system Hilbert space is two-dimensional. The results of the dimensional comparison are given in the following figure.

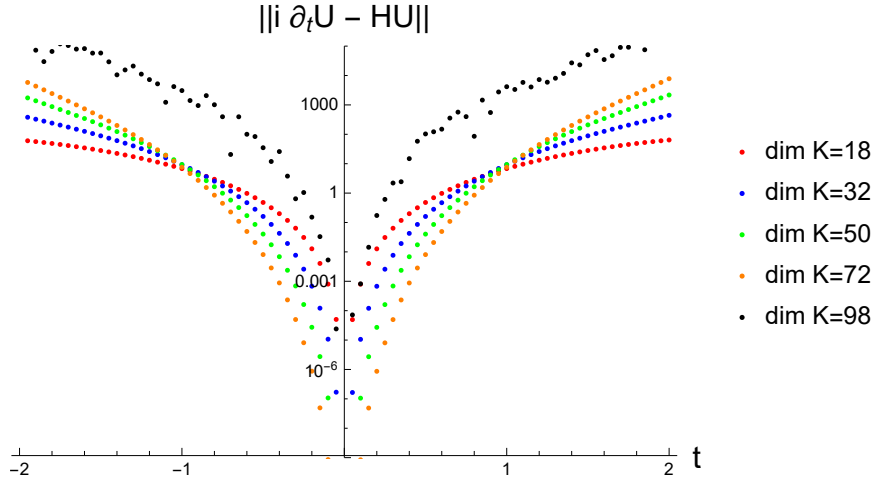


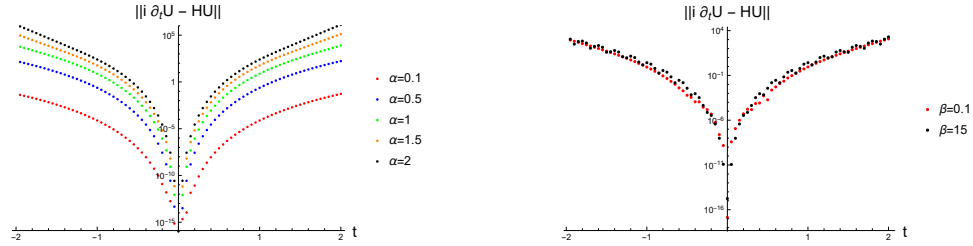
Figure 3.4.: Depicted is the norm of the Schrödinger equation $\|i\partial_t U(t) - H(t)U(t)\|$ for different times and different dimensions of \mathcal{K} . The system parameters were fixed as $\alpha = 1$ and $\beta = 1$. The norm of the Schrödinger equation immediately increases with time. There is no 'breaking point'. The greater the dimension the smaller the norm for a fixed time value however. This implies that the dimensions included in the calculations so far are too small to display the plateau seen in Fig. 3.1

The results greatly differ from those depicted in Fig. 3.1. There is no 'breaking point', instead the size of $\|i\dot{U}(t) - H(t)U(t)\|$ immediately increases quite sharply and follows an approximately exponential curve for times greater than $t \approx 0.8$. While for short times larger dimensions of \mathcal{K} have smaller errors, this behaviour reverses for larger

3. Application of generalized Floquet theory

times as the steepness of the exponential part is greater for greater dimensions. Also the highest dimension included in the calculations so far produced by far the worst results. This behaviour seems very counter-intuitive at first but can be explained by the interpolation formula used (Eq. (2.44)). For large multiplicities of an eigenvalue the denominator of Eq. (2.44) includes terms with very high powers, if additionally two or more eigenvalues are very close, the denominator can easily take values of magnitudes 10^{-100} and smaller. This probably leads to a breakdown in the numerical calculations and the interpolation formula fails for all higher dimensions. It should also be mentioned however, that the dimensions of \mathcal{K} considered so far are of the same order as magnitude as the ones included in the calculations for the Schrödinger picture Hamiltonian even though we now have to truncate for two indices. This means that the part of the extended Hilbert space included in the calculations is much smaller (in relation to the total size of the Hilbert space) for the interaction picture Hamiltonian, so it is very likely that we simply have not included enough functions to see the 'breaking point'. It has not been possible to include sufficiently high dimensions to test the influence of this yet, as the computation time again increases exponentially with the dimension and the interpolation breaks down for high dimensions as mentioned before.

To test the dependence of the propagator on the system parameters we fixed the dimension of \mathcal{K} as $\dim[\mathcal{K}] = 72$ (corresponding to $y = 6$), as this is the highest dimensions with reasonable results accessible at the moment.



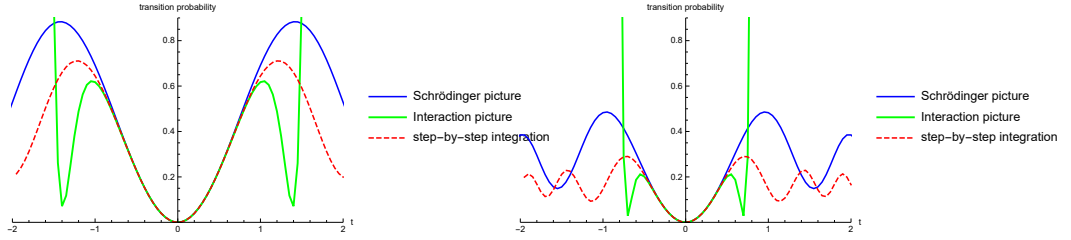
(a) The dependence of the propagator $U(t)$ on different values of α is examined. The second parameter is fixed ($\beta = 1$). The smaller the value of α , the smaller the norm. This implies that the generalized Floquet formalism is best suited for the treatment of a small time-dependent term. The interesting time-regime however is given by $|\alpha t| \gg \beta$. The range of α values accessible with the interaction picture Hamiltonian is smaller than that for the Schrödinger picture Hamiltonian.

(b) The dependence of the propagator $U(t)$ on different values of β is examined. The second parameter is fixed ($\alpha = 1$). While α has a strong influence on the quality of the propagator, β has again no meaningful influence on the norm of the Schrödinger equation.

Figure 3.5.: Depicted is the dependence of the time-evolution operator on the system parameters. All calculations were done for $\dim[\mathcal{K}] = 72$. On the left α is varied and on the right it is β .

3. Application of generalized Floquet theory

Again the error greatly increases with increasing α . Whereas for the Schrödinger picture Hamiltonian we could include values of α with $\alpha > \beta$, this is not possible in this case. Therefore the regime $|\alpha t| \gg \beta$ is inaccessible for the interaction picture representation, at least for the dimension used so far. As for the β -dependence, the behaviour is very similar to the behaviour depicted in Fig. 3.2(b). The error is almost completely unaffected by the choice of β . Only for very large values of β does the error decrease slightly. This behaviour seems reasonable, as we already noted that both computations work the best if $\beta > |\alpha t|$. The β -dependence was tested for $\alpha = 1$ and for the α -dependence we fixed $\beta = 1$, same as for the Schrödinger picture case. In the last part of this section we compare transition rates obtained using the two different representations of the Landau-Zehner Hamiltonian with a numerical integration of the Schrödinger equation for the interaction picture Hamiltonian.



(a) The system parameters are set to $\alpha = 0.5$ and $\beta = 1$. For the Schrödinger picture calculation the dimension is 80, for the interaction picture it is 72. In this setting the three transition probabilities agree very well up to $t \approx 1$ afterwards the transition rates deviate. The time-independent approach for the interaction picture Hamiltonian completely breaks down for $t = 1.4$.

(b) The system parameters are set to $\alpha = 2$ and $\beta = 1$. For the Schrödinger picture calculation the dimension is 80, for the interaction picture it is 72. In this setting the three transition probabilities agree up to only $t \approx 0.35$. For times greater than $t = 0.7$ the interaction picture results again break down completely.

Figure 3.6.: Transition probabilities $|\langle 1|U(t,0)|0\rangle|^2$ computed using the generalized Floquet formalism for the Schrödinger picture Landau-Zehner Hamiltonian and the interaction picture Landau-Zehner Hamiltonian are compared with values obtained by numerically integrating the time-dependent Schrödinger equation for the interaction picture Hamiltonian.

For small times the three transition probabilities agree very well. The time scale for which this statement holds true strongly depend on the choice of α . The larger α , the shorter the time.

After the transition probabilities begin to deviate, the time-independent formalism breaks down for the interaction picture Hamiltonian and the corresponding transition rates become unphysically large ($|\langle 1|U(t,0)|0\rangle|^2 > 1$). While this behaviour is not unexpected considering the results from Fig. 3.4 and Fig. 3.5(a), it is problematic that the results from the numerical integration and the Schrödinger picture calculation do

3. Application of generalized Floquet theory

not agree for the whole time interval. It should especially be noted, that the oscillation of the transition probability is faster for the numerical integration in Fig. 3.6(b) and that the absolute value of the transition probability is smaller in both cases after the three transition rates split. This behaviour could not be observed in Fig. 3.3, where we depicted the results from the numerical integration of the Schrödinger picture Hamiltonian. This indicates, that also the numerical integration of the Schrödinger equation with the interaction picture Hamiltonian is not as unproblematic as it was for the Schrödinger picture Hamiltonian. As this behaviour was noticed only recently a more thorough study of the problem has not been possible as of yet.

3.3. Hamiltonian with Gaussian perturbation

The last model Hamiltonian considered in this thesis describes a two-level system coupled to an external perturbation, inducing a transition between the two levels,

$$H(t) = \frac{\omega}{2} \sigma_z + \Omega e^{-\frac{\alpha}{2} t^2} \sigma_x. \quad (3.14)$$

The perturbation has a Gaussian time-dependence and couples to the system with coupling strength Ω , α is a positive real number characterising the Gaussian function (eg. the pulse width) and ω describes the energy separation of the system. Let us first rewrite the Hamiltonian in a more convenient form

$$H(t) = \Omega \left(\frac{\omega'}{2} \sigma_z + e^{-\frac{\alpha'}{2} t'^2} \sigma_x \right) \quad (3.15)$$

where we defined $\omega' = \frac{\omega}{\Omega}$, $\alpha' = \frac{\alpha}{\Omega^2}$ and $t' = \Omega t$. All the primed parameters are dimensionless.

For all further discussions we will use $H(t) = (\frac{\omega}{2} \sigma_z + e^{-\frac{\alpha}{2} t^2} \sigma_x)$, where we dropped the prime notation out of convenience. This implies that when we change the coupling strength to $\Omega_{new} = x\Omega$ the same dynamics are obtained if we change all the parameters accordingly, $\omega_{new} = x\omega$, $t_{new} = t/x$ and $\alpha_{new} = x^2\alpha$.

For this Hamiltonian the time-dependent functions take the form

$$f_{pq}(t) = t^p e^{-q \frac{\alpha}{2} t^2} \quad (3.16)$$

with $p, q \in \mathbb{N}$.

Again we introduce the appropriate Floquet space $\mathcal{F} = \mathcal{H}_S \otimes \mathcal{T}''$. Here \mathcal{T}'' is constructed by associating the time-dependent functions $f_{pq}(t)$ with the basis states $|f_{pq}\rangle$ of an infinitely dimensional space. This allows us to again express the Schrödinger operator as a time-independent operator in the extended Hilbert space

$$\mathcal{K} = \frac{\omega}{2} \sigma_z \otimes \mathbb{1} + \sigma_x \otimes a_q^\dagger - i(a_p \otimes \mathbb{1} - \alpha b_p^\dagger \otimes \mathbb{1}). \quad (3.17)$$

3. Application of generalized Floquet theory

The raising and lowering operators are defined by their action on the basis elements of the space of time-dependent functions \mathcal{T} :

$$\begin{aligned} a_q^\dagger |f_{pq}\rangle &= |f_{p(q+1)}\rangle \\ b_p^\dagger |f_{pq}\rangle &= q |f_{(p+1)q}\rangle \\ a_p |f_{pq}\rangle &= p |f_{(p-1)q}\rangle. \end{aligned} \quad (3.18)$$

As before we define these operators in accordance with the action of the time-dependent part of the Hamiltonian and the time-derivative operator on the time-dependent functions associated with the state vectors:

$$\begin{aligned} e^{-\frac{\alpha}{2}t^2} f_{pq}(t) &= f_{p(q+1)}(t) \\ \frac{\partial}{\partial t} f_{pq}(t) &= p f_{(p-1)q}(t) - \alpha q f_{(p+1)q}(t). \end{aligned} \quad (3.19)$$

In the following section we will again examine the properties of the time-evolution operator calculated using Eq. (3.13), but this time we use the time-dependent functions introduced in Eq. (3.15) and the matrix exponential of the time-independent Schrödinger operator introduced in Eq. (3.16).

3.3.1. Numerical results

The time-dependent functions have a similar structure to those introduced for the treatment of the interaction picture Landau-Zehner Hamiltonian. Here however the exponential function is of a Gaussian-type, while before we had complex exponential functions. As we limited ourselves to positive real values of α the exponential term should facilitate the treatment of large times. The time-dependent functions are again subject to two different indices, so following the procedure introduced for the interaction picture Landau-Zehner Hamiltonian we defined a parameter y and included all values of p and q satisfying $p + q \leq y$ in our calculations. As before we first analyse the influence of the truncation on the propagator for fixed system parameters $\alpha = 1$ and $\omega = 5$. The results are depicted in Fig. 3.7.

Once again we note that the more dimensions of \mathcal{F} are included in the calculations, the better does the obtained propagator solve the Schrödinger equation. The differences are not as pronounced as for the Landau-Zehner Hamiltonian however. For large times ($t > 1.5$) the norm becomes the same regardless of the dimension. This is most likely due to the influence of the Gaussian term. Unlike for the Schrödinger picture Landau-Zehner Hamiltonian there is no plateau. Instead, the norm of the Schrödinger equation increases with time regardless of the value of the time parameter. Here however the error is capped at $\|i\dot{U}(t) - H(t)U(t)\| \approx 1$, while there seems to be no cap for the interaction picture Hamiltonian. As pointed out before this is probably due to the Gaussian term instead of the complex exponential. Due to the exponentially increasing computational time (see Sec. 3.4) we can only include a very small number of y -values in our calculations ($y_{max} = 7$). It is desirable to

3. Application of generalized Floquet theory

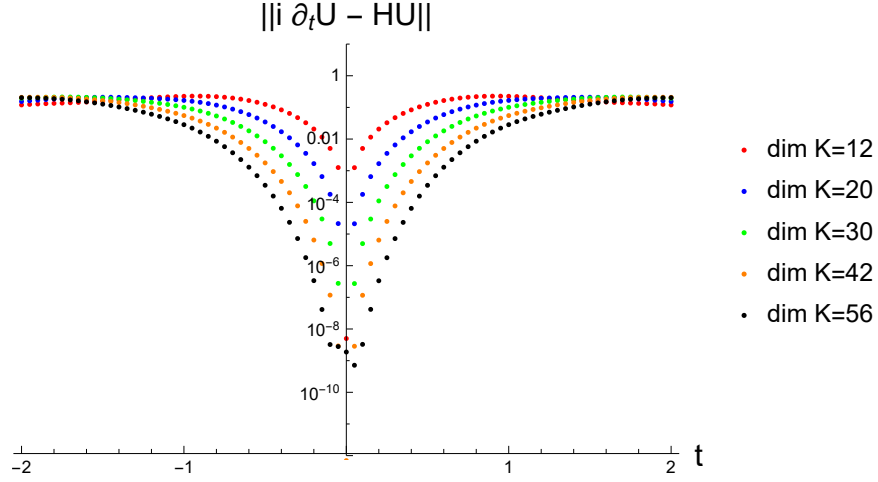


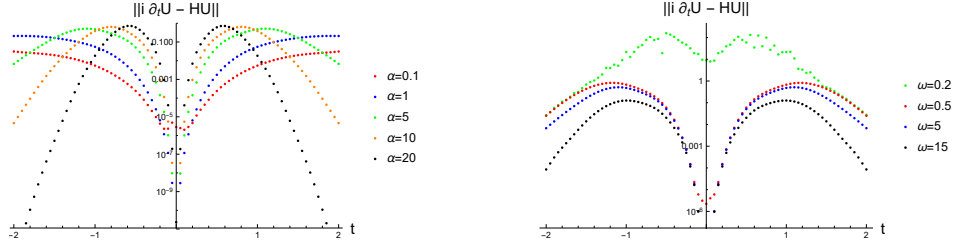
Figure 3.7.: Depicted is the norm of the Schrödinger equation $\|i\dot{U}(t) - H(t)U(t)\|$ for different times and different dimensions of \mathcal{K} . The system parameters were fixed as $\alpha = 1$ and $\omega = 5$. The norm of the Schrödinger equation immediately increases with time. There is no 'breaking point'. The greater the dimension the smaller the norm for a fixed time value however. This implies that the dimensions included in the calculations so far are again too small to display the plateau seen in Fig. 3.1. The norm never gets larger than 1, because of the Gaussian-type exponential functions. This behaviour could not be observed in Fig. 3.4, where the norm would reach values of up to 10^4 .

greatly increase this value in order to even come close to including a similar portion of the Hilbert space as in the calculations for the Schrödinger picture Landau-Zehner Hamiltonian.

For the second part we again discuss the influence of the system parameters. For the following calculations we fixed $y = 6$ ($\dim[\mathcal{K}] = 42$) and first varied α for constant $\omega = 5$ and afterwards ω for $\alpha = 1$. The results are depicted in Fig. 3.8.

While the norm increases more quickly for larger values of α at first it reaches a maximum and afterwards decreases again for larger times. The larger α the faster the maximum error is reached and the faster does the error decrease afterwards. This behaviour only occurs for $\alpha > 1$. It can be attributed to the exponential term in the Hamiltonian tending to zero for large values of αt^2 . As for the other two Hamiltonians the prefactor of the time-independent term does not influence the norm much. This statement does not hold true for very small values of ω however as this implies small eigenvalues of \mathcal{K} which leads to a breakdown of the interpolation formula (Eq. 2.44). This behaviour is similar to the behaviour discussed in Sec. 3.2.2 for the interaction picture Landau-Zehner Hamiltonian for large dimensions or small values of β .

3. Application of generalized Floquet theory



- (a) The dependence of the propagator $U(t)$ on different values of α is examined. The second parameter is fixed ($\omega = 5$). The greater the value of α , the faster the increase of the norm of the Schrödinger equation. For $\alpha > 1$ the norm reaches a maximum and decreases for larger times. The maximum is reached faster for larger values of α and the subsequent decrease is also faster. This behaviour reflects the influence of the Gaussian-type exponential functions.
- (b) The dependence of the propagator $U(t)$ on different values of ω is examined. The second parameter is fixed ($\alpha = 5$). The norm of the Schrödinger equation is smaller for larger values of ω . The general shape of the curves is similar for all values of ω , except for the smallest. Here the interpolation formula breaks down.

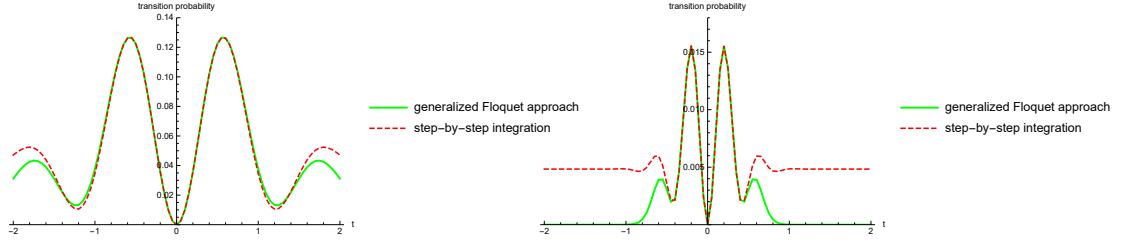
Figure 3.8.: Depicted is the dependence of the time-evolution operator on the system parameters. All calculations were done for $\dim[\mathcal{K}] = 42$. On the left α is varied and on the right it is ω .

For the Schrödinger picture Hamiltonian this behaviour is not observed, because there every eigenvalue occurs only once and Silvester interpolation can be used instead of Hermite interpolation.

In the last part we again discuss transition probabilities. The results are depicted in Fig. 3.9.

The transition probabilities computed for this Hamiltonian agree well with the results from the numerical integration for $\alpha = 1$, considering that the calculations could only be done for a very small dimension, $\dim[\mathcal{K}] = 42$. Nonetheless, the results are in way better agreement than for the interaction picture Landau-Zehner Hamiltonian. This is due to the fact, that the time-dependent functions in this case contain an exponential function of Gaussian type, which allows for a better treatment of large times than the complex exponential used for the interaction picture Landau-Zehner Hamiltonian. Again we are however confronted with the fact, that it is only possible to include a very small portion of Floquet space in the calculations. This is the main issue with the performance of the generalized Floquet formalism, same as for the two previous Hamiltonians.

3. Application of generalized Floquet theory



- (a) The system parameters are set to $\alpha = 1$ and $\omega = 5$. The transition probabilities agree very well up to $t = 1.6$. Afterwards the results obtained with the generalized Floquet approach are slightly smaller.
- (b) The system parameters are set to $\alpha = 10$ and $\omega = 15$. The transition probabilities only agree up to $t = 0.4$. Afterwards the transition probabilities calculated using the generalized Floquet approach quickly drop down to zero, while the results from step-by-step integration become constant as well but they are non-vanishing.

Figure 3.9.: Transition probabilities $|\langle 1|U(t,0)|0\rangle|^2$ computed using the generalized Floquet formalism for the Hamiltonian with a Gaussian perturbation are compared with values obtained by numerically integrating the time-dependent Schrödinger equation.

For $\alpha = 10$ the transition probabilities agree only for a very short time scale ($-0.4 < t < 0.4$). Afterwards the transition probabilities calculated using the generalized Floquet approach drop down to zero, while the results from the numerical integration remain small but non-vanishing. The shape of the two graphs is very similar however. Considering the structure of the Hamiltonian, one expects the transition probability to become constant for $\alpha t^2 \gg 1$, as the time-dependent term responsible for the transition vanishes in this case and the transition probability will not change anymore. A sudden drop in the transition probability down to zero however is unreasonable for a non-vanishing transition probability for the previous time values. This implies that the propagator, calculated using the generalized Floquet approach, does not correctly describe the system dynamics for large times even though the norm of the Schrödinger equation would suggest that the propagator improves again for larger times after the norm reaches a maximum (see Fig. 3.8(a)). The transition probability in Fig. 3.9(b) drops down to zero right after the norm passes the maximum point however. In this case the norm of the Schrödinger equation is misleading as a measure of quality.

3.4. Computational time

In this section we consider the computational time needed to calculate the propagator $U(t, 0)$ for the three time-dependent Hamiltonians introduced in the previous sections. While the absolute physical time required for the calculations is computer-dependent it still shows how the time scales up with the dimensions of the calculation.

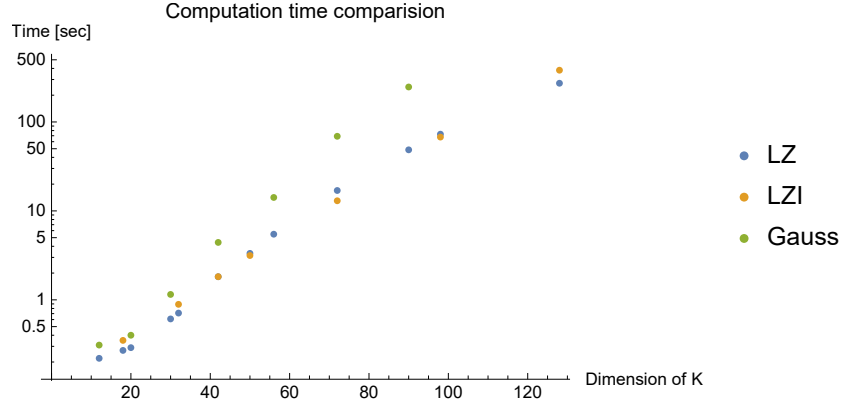


Figure 3.10.: *Depicted is the physical time required to calculate the propagator $U(1, 0)$ for the three different model Hamiltonians for various dimensions. The time increases exponentially for all three Hamiltonians. The Gaussian-Hamiltonian ('Gauss') requires the most time, while for the two Landau-Zehner Hamiltonians ('LZ' and 'LZI', for the interaction picture) the time is of the same size.*

As seen in Fig. 3.10 the time scales up exponentially with the dimensions of the problem for all three model Hamiltonians. The run-times for the two Landau-Zehner Hamiltonians are of the same order of magnitude, while the Gauss-Hamiltonian takes longer. The biggest contribution to the run-time ($\approx 90\%$) of the Landau-Zehner Hamiltonian in Schrödinger picture comes from the calculation of the eigenvalues of \mathcal{K} while for the other two Hamiltonians it is the calculation of the terms needed for Hermite interpolation (Eq. (2.44)) that takes up the most time. This is problematic as the interpolation has to be done anew for every point in time. The eigenvalues however have to be determined only once. Therefore the Landau-Zehner Hamiltonian in Schrödinger picture allows to calculate the propagator for different times far more efficiently than the other two Hamiltonians. The problem for them being a large multiplicity of certain eigenvalues. To tackle this problem and also the problem of the propagators displaying unphysical behaviour after the dimensions of \mathcal{K} are increased beyond a certain point, the maximal multiplicity of the eigenvalues could be fixed and all copies of eigenvalues exceeding the threshold would simply be discarded in the calculations. While this idea has not been sufficiently tested as of yet, first results were promising.

3. Application of generalized Floquet theory

It should be noted, that the numerical integration of the time-dependent Schrödinger equation and the subsequent calculation of the time-evolution operator $U(t_1, 0)$ for a certain point in time $t = t_1$ can be done in under 5 seconds for all three model Hamiltonians and the time interval $t_1 \in [-2, 2]$, therefore being much more efficient than the generalized Floquet approach at this stage.

4. Conclusion and Outlook

A generalization of the time-independent Floquet method has been applied to three model Hamiltonians from molecular and optical physics with a non-periodic time-dependence. For every Hamiltonian the extended Hilbert space (Floquet space \mathcal{F}) is constructed through addition of the space of the relevant time-dependent functions and the Schrödinger operator $K(t)$ is transformed into an effectively time-independent operator \mathcal{K} on the extended space. Using the matrix exponential $e^{-i\mathcal{K}t}$ the time-evolution operator $U(t,0)$ is calculated for the three systems. Because the operator \mathcal{K} is non-hermitian for all systems considered so far the matrix exponential has to be calculated using interpolation formulas.

The numerical dependence of the time-evolution operator on the system parameters and the dimension of \mathcal{F} included in the calculations is investigated. While the results for the Landau-Zehner Hamiltonian in the Schrödinger picture representation are promising, the method is at this state basically useless for the other two Hamiltonians (Interaction picture Landau-Zehner and Hamiltonian with Gaussian time-dependence). The time-scale for which the algorithm produces sensible results are so short, that both perturbation theory as well as a Taylor expansion of the matrix exponential can be used with far less computational effort. The main problem of the whole approach is the exponential increase in computation time with increasing dimension of \mathcal{F} . This greatly limits the number of time-dependent functions included in the calculations and this in turn introduces the greatest error in the calculation of the time-evolution operator. This problem is especially prominent for the two latter Hamiltonians, where the time-dependent functions depend on two indices but it is for this reason so far also impossible for the Schrödinger picture Landau-Zehner Hamiltonian to fully access the time-regime of interest ($|\alpha t| \gg \beta$).

To tackle this problem a two option approach should be mentioned. First of all one could develop a more efficient interpolation algorithm and thus increase the number of accessible dimensions. The second option is to use a different set of time-dependent functions, preferably such that \mathcal{K} is hermitian on the extended Hilbert space.

All in all the generalized time-independent Floquet formalism works in principle, however the numerical realisation is still lacking in many aspects. So far the formalism can not be considered to be a viable alternative to the standard procedure of numerically integrating the time-dependent Schrödinger equation in terms of its practical usefulness. There are however still the above mentioned avenues to explore in order to possibly improve the performance of the generalized Floquet formalism and turn it into a viable tool for the treatment of time-dependent quantum systems. Another question of interest is whether it is possible to derive analytic expressions for the time-evolution operator using Eq. (2.31) in the limit of very long times. First exploits

4. Conclusion and Outlook

in this direction have proven fruitless but a more thorough discussion is required to answer this question satisfactory.

A. Appendix

A.1. Propagator for the Landau-Zehner Hamiltonian

In this section we will show that the time-evolution operator $U(t, 0) = \sum_n t^n \langle n | e^{-i\mathcal{K}t} | 0 \rangle$ satisfies the time-dependent Schrödinger equation $i\partial_t U(t, 0) = (\beta\sigma_x + \alpha t\sigma_z)U(t, 0)$ with the initial condition $U(0, 0) = \mathbb{1}$. The Schrödinger operator in Floquet space (see Sec. 3.1) is given by

$$\mathcal{K} = \beta\sigma_x \otimes \mathbb{1} + \alpha\sigma_z \otimes a^\dagger - i\mathbb{1} \otimes a. \quad (\text{A.1})$$

Let us consider the time-derivative of the propagator

$$\begin{aligned} i\partial_t U(t) &= \sum_n \left(int^{n-1} \langle f_n | \mathcal{V} | f_0 \rangle + it^n \langle f_n | - i\mathcal{K} \mathcal{V} | f_0 \rangle \right) \\ &= \sum_n \left(int^{n-1} \langle f_n | \mathcal{V} | f_0 \rangle + t^n \langle f_n | (\beta\sigma_x \otimes \mathbb{1} + \alpha\sigma_z \otimes a^\dagger - i\mathbb{1} \otimes a) \mathcal{V} | f_0 \rangle \right) \\ &= \sum_n \left(int^{n-1} \langle f_n | \mathcal{V} | f_0 \rangle + t^n \beta\sigma_x \langle f_n | \mathcal{V} | f_0 \rangle + \alpha\sigma_z t^n \langle f_{n-1} | \mathcal{V} | f_0 \rangle - i(n+1)t^n \langle f_{n+1} | \mathcal{V} | f_0 \rangle \right) \\ &= \sum_n \left(t^n \beta\sigma_x \langle f_n | \mathcal{V} | f_0 \rangle + \alpha\sigma_z t^{n+1} \langle f_n | \mathcal{V} | f_0 \rangle \right) \\ &= (\beta\sigma_x + t\alpha\sigma_z) \sum_n t^n \langle f_n | \mathcal{V} | f_0 \rangle \\ &= H(t)U(t). \end{aligned} \quad (\text{A.2})$$

Here we used $\langle f_n | a^\dagger = \langle f_{n-1} |$ and $\langle f_n | a = (n+1) \langle f_{n-1} |$ and shifted the index of summation in such a way that every term includes $\langle f_n | \mathcal{V} | f_0 \rangle$. Also the condition $U(0) = \mathbb{1}$ is satisfied, because $U(0) = \sum_n f_n(t) \langle f_n | \mathbb{1} | f_0 \rangle = \mathbb{1}$.

A.2. Landau-Zehner Hamiltonian in interaction picture

In this section we derive the interaction picture representation of the Landau-Zehner Hamiltonian introduced in Sec. 3.2. In the Schrödinger picture the Hamiltonian is given by

$$H(t) = \beta\sigma_x + \alpha\sigma_z t. \quad (\text{A.3})$$

To get the interaction picture representation we write the Hamiltonian as

$$H(t) = H_1 + H_2 \quad (\text{A.4})$$

with $H_1 = \beta\sigma_x$ and $H_2 = H_2(t) = \alpha t\sigma_z$. We have $[H_2(t_1), H_2(t_2)] = 0$ so the time-evolution operator for $H_2(t)$ is given simply by $U_{H_2}(t) = e^{-iH_2 t}$. The interaction

A. Appendix

picture Hamiltonian can then be calculated as

$$H_I(t) = e^{iH_2t} H_1 e^{-iH_2t}. \quad (\text{A.5})$$

Let us rewrite the right-hand side of Eq. (A.5):

$$\begin{aligned} \beta e^{i\alpha t^2 \sigma_z} \sigma_x e^{-i\alpha t^2 \sigma_z} &= \beta (\cos(\alpha t^2) + i \sin(\alpha t^2) \sigma_z) \sigma_x (\cos(\alpha t^2) - i \sin(\alpha t^2) \sigma_z) \\ &= (\cos^2(\alpha t^2) - \sin^2(\alpha t^2)) \sigma_x - 2 \cos(\alpha t^2) \sin(\alpha t^2) \sigma_y \\ &= \frac{\beta}{2} (2 \cos(2\alpha t^2) \sigma_x - 2 \sin(2\alpha t^2) \sigma_y) \\ &= \frac{\beta}{2} (\sigma_+ e^{2i\alpha t^2} + \sigma_- e^{-2i\alpha t^2}). \end{aligned} \quad (\text{A.6})$$

Here the last line gives the desired expression for the interaction picture Hamiltonian with $\sigma_{\pm} = \sigma_x \pm i\sigma_y$. To derive this result we used $e^{i\alpha A} = (\cos(\alpha) + i \sin(\alpha) A)$ for $A^2 = \mathbb{1}$ (A being an operator on Hilbert space), the commutation relation between the Pauli operators $[\sigma_i, \sigma_j] = i\varepsilon_{ijk} \sigma_k$ and the trigonometric relations $\cos(2x) = \cos^2(x) - \sin^2(x)$ and $\sin(2x) = 2 \cos(x) \sin(x)$.

Bibliography

- [1] Lloyd S, 1996, ‘Universal Quantum Simulators’, *Science*, 273:5278
- [2] Feynman R P, 1986, ‘Quantum Mechanical Computers’, *Found. Phys.*, 16:507
- [3] Braun S, Ronzheimer J P, Schreiber M, Hodgman S S, Rom T, Bloch I and Schneider U, 2013, ‘Negative Absolute Temperature for Motional Degrees of Freedom’, *Science*, 339:52
- [4] Jotzu G, Messer M, Desbuquois R, Lebrat M, Uehlinger T, Greif D and Esslinger T, 2014, ‘Experimental Realization of the Topological Haldane Model with Ultracold Fermions’, *Nature*, 515:237
- [5] Ray M W, Ruokokoski E, Tiurev K, Möttönen M and Hall D S, 2015, ‘Observation of Isolated Monopoles in a Quantum Field’, *Science*, 348:544
- [6] Shapiro M and Brumer P, 1994, ‘Coherent and Incoherent Laser Control of Photochemical Reactions’, *Int. Rev. Phys. Chem.*, 13:187
- [7] Becker W, Liu X, Ho P J and Eberly J H, 2012, ‘Theories of Photoelectron Correlation in laser-driven Multiple Atomic Ionization’, *Rev. Mod. Phys.*, 84:1011
- [8] Tokura Y, 2006, ‘Photoinduced Phase Transition: A Tool for Generating a Hidden State of Matter’, *J. Phys. Soc. Jap.*, 75:011001
- [9] Cirac J I and Zoller P, 2012, ‘Goals and Opportunities in Quantum Simulation’, *Nat. Phys.*, 8:264
- [10] Floquet G, 1883, ‘Sur les Equations Differentielles Lineaires a Coefficients Periodiques’, *Ann. Ecole Norm. Sup.*, 12:47
- [11] Ho T-S, Chu S-I and Tietz J V, 1983, ‘Semiclassical many-mode Floquet Theory’, *Chem. Phys. Lett.*, 96:464
- [12] Vilalta A V, Puig J and Mintert F, 2016, ‘Quasi-periodically Driven Quantum Systems’, *arXiv:1603.03923*
- [13] Vilalta A V, 2015, ‘Optimally Driven Quantum Systems’, *Unpublished PhD Thesis*, Imperial College London
- [14] Shirley J H, 1965, ‘Solution of the Schrödinger Equation with a Hamiltonian Periodic in Time’, *Phys. Rev.*, 138:B979
- [15] Sambe H, 1973, ‘Steady States and Quasienergies of a Quantum-mechanical System in an Oscillating Field’, *Phys. Rev. A*, 7:2203
- [16] Howland J S, 1974, ‘Stationary Scattering Theory for time-dependent Hamiltonians’, *Math. Ann.*, 207:315

Bibliography

- [17] Hänggi P, 1998, ‘Driven Quantum Systems’, *Quantum Transport and Dissipation*. (Wiley-VCH, Weinheim, 1998), 1998:249-86
- [18] Peskin U and Moiseyev N, 1993, ‘The Solution of the time-dependent Schrödinger Equation by the (t,t') Method: Theory, Computational Algorithm and Applications’, *J. Chem. Phys.*, 99:4590
- [19] Moler C and van Loan C, 2003 ‘Nineteen Dubious Ways to Compute the Exponential of a Matrix, twenty-five years later’, *SIAM review*, 45:1
- [20] Higham N J, 2008 ‘Functions of Matrices: Theory and Computation’, <http://dx.doi.org/10.1137/1.9780898717778>, University of Manchester
- [21] Sylvester J J, 1883, ‘On the Equation to the Secular Inequalities in the Planetary Theory’, *Philos. Mag.*, 16:267
- [22] Friedman B, 1956, ‘Principles and Techniques of Applied Mathematics’, *Wiley*
- [23] Jeffreys H and Jeffreys B S, 1998, ‘Lagrange’s Interpolation Formula’, *Methods of Mathematical Physics*, *Cambridge University Press*, 1998:260
- [24] Hamilton W R, 1864, ‘On the Existence of a Symbolic and Biquadratic Equation, which is satisfied by the Symbol of Linear Operation in Quaternions’, *Proceedings of the Royal Irish Academy*, *Royal Irish Academy*, 7:190
- [25] Buchheim A, 1886, ‘An Extension of a Theorem of Prof. Sylvester Relating to Matrices’, *Philos. Mag.*, 22:173-174
- [26] Marcus M and Ming H, 1964, ‘A Survey of Matrix Theory and Matrix Inequalities’, *Allyn and Bacon*
- [27] Rinehart R F, 1955, ‘The Equivalence of Definitions of a Matrix Function’, *American Math Monthly*, 62:395-414
- [28] Landau L, 1932, ‘Zur Theorie der Energieübertragung. II’, *Physikalische Zeitschrift der Sowjetunion*, 2:46-51
- [29] Zener C, 1932, ‘Non-adiabatic Crossing of Energy Levels’, *Proceedings of the Royal Society of London A*, 137:696-702